

EUROFEL-Report-2007-DS2-088

EUROPEAN FEL Design Study



Deliverable N°: D 2.9

Deliverable Title: Evaluate the limitations on high current operation for 4GLS and Arc-en-Ciel operation - BBU Limitations for 4GLS and Arc-en-Ciel

Task: DS-2

Authors: see next page

Contract N°: 011935

**Project funded by the European Community
under the “Structuring the European Research Area” Specific Programme
Research Infrastructures action**

BBU Limitations for 4GLS and Arc-en-Ciel

E. Wooldridge, B. Muratori, H. Owen, S. Smith, ASTeC, Daresbury Laboratory
C. Bruni, A. Loulergue, M. E. Couprie, Synchrotron SOLEIL

Abstract

The designs for 4GLS and Arc-en-Ciel contain an Energy Recovery Linac (ERL) and a beam current of 100mA accelerated to 550 MeV and 2 GeV respectively. This will be challenging with regards to beam stability, since the interaction with the beam and any Higher Order Modes (HOMs) contained within the cavity could lead to the beam being lost, due to the collective effect known as Beam Break-Up (BBU). This report will discuss the linac quadrupole focusing schemes for both machines, which for one pass are similar. It will also look at the two-pass case required for 2GeV operation at Arc-en-Ciel. Further refinement of these focusing schemes will be discussed and for a multi-cavity system we will show the values of R22 and R44 must be considered in addition to the R12 and R34 given by the single cavity equation. The energy of the beam injected into the ERL linac will be shown to be an important factor in increasing the threshold, and we will present a seven-cell cavity design that increases the peak BBU threshold current by 50%. The requirement of 100 mA BBU threshold current for both Arc-en-Ciel and 4GLS has been met; However, this is for a small parameter space, and future work detailing how this parameter space may be increased is discussed.

1. Introduction

The high current designs of 4GLS and Arc-en-Ciel provide interesting challenges with regards to beam stability. Both designs consist of Energy Recovery Linacs (ERLs) where high average current beams of the order of 100 mA will be accelerated to high energy - 550 MeV and 2 GeV for 4GLS and Arc-en-Ciel respectively, in picosecond-scale bunches. A collective effect known as Beam Break-Up (BBU) arises from a feedback between the accelerating and decelerating electron bunches and the RF cavities. An initial offset in the incoming bunches may be amplified under certain conditions, grow exponentially, and therefore lead to beam loss. This can limit the average current in the ERL, the limit above which exponential growth occurs being known as the threshold current.

BBU results from the interaction of excited Higher Order Modes (HOMs) with the beam. These HOMs are excited by a transversely-shifted beam and/or cavity misalignments, and the transverse force due to the resulting wakefield can modify the momentum of the following bunches. Consequently the choice of optics and element arrangement is of great importance in minimising this instability.

The problem of BBU has been separated into two parts in this study: the focusing of the accelerating and decelerating beams within the main linac and the effect of the cavity geometry; and the recirculation from the end of the linac after the beam has been accelerated to the beginning of the linac before the beam is decelerated. The choice of focusing scheme throughout the linac will be of importance to avert beam break-up and this paper will look at the focusing scheme solely on this issue, ignoring other effects this will have on the lattice. Methods of decreasing the Higher Order Mode (HOM) Q, quality factor, and R/Q will be important factors, as will the phase advance. Each of these points will be discussed in turn.

1.1 Machine definitions

1.1.1 4GLS

The design for 4GLS has two parts:

- a High Average Current Loop (HACL) forms the ERL where the beam will pass through 5 superconducting modules, each containing eight 7-cell cavities, with 77 pC bunches to accelerate the beam from 10 MeV to 550 MeV (see fig.1).
- a second part where 1 nC bunches are accelerated through the same linac with a repetition rate of 1 kHz. These accelerating bunches will be interlaced with the ERL ones.

Regenerative multipass BBU is an average current phenomenon (see below) therefore it is important that the BBU current threshold of the machine is greater than the sum of these two currents. The effects of the wakefields from the XUV-FEL bunches are small enough that they do perturb the energy of the following HACL bunches greatly [7].

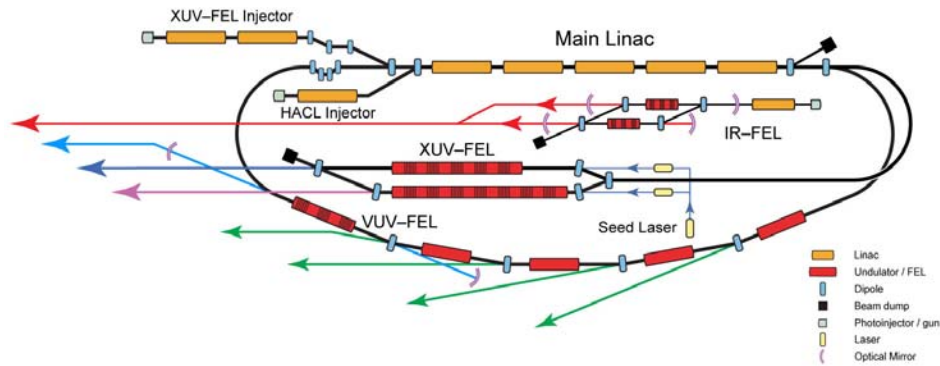


Figure 1: Schematic representation of the 4GLS facility, which includes the ERL considered in this study.

1.1.2 Arc-en-Ciel

The Arc-en-Ciel project comprises an ERL configuration based on a 1 GeV linac with either one or two recirculations, with 1 to 100 mA average current (1 nC, and 1 to 100 MHz repetition rate). It is composed of a linac, bunch compressor and 3rd-harmonic linearising cavity system. The first compressor is in the injection section, whereas the second is within the ERL loop. For stability reasons, the second chicane will be bypassed as the beam is injected. The ERL is composed of a 1 GeV Linac and two recirculation loops to reach a final energy of 2 GeV (see fig.2).

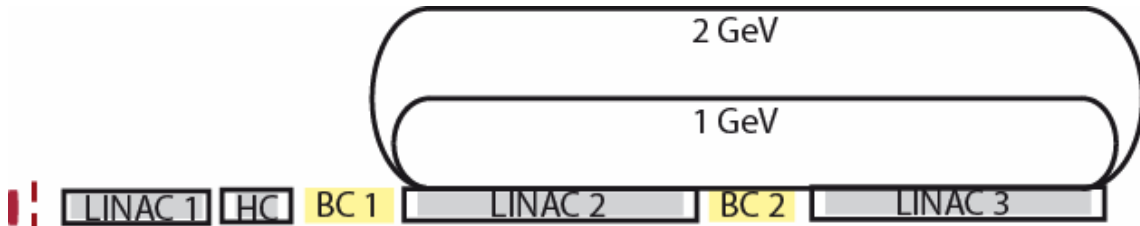


Figure 2: Representation of the Arc-en-Ciel ERL. LINAC: Linear accelerator composed of cryomodules, HC: third harmonic cavity, BC: bunch compressor (not to scale). The linac is 200 m long and the radius of the arcs is 15 and 30 meters.

2 BBU modelling

For a single cavity with a single higher-order mode (HOM) and one-pass recirculation, the threshold current may be given by the analytical formula [1,2,3,6,11]

$$I_{th} = \frac{-2p_r}{e \left(\frac{R}{Q} \right)_m Q_m k_m R_{ij} \sin(\omega_m t_r)} , \quad (1)$$

where $(R/Q)_m$ and Q_m are the shunt impedance and quality factor for the transverse higher order mode (HOM) m , with frequency ω_m , $k_m = \omega_m/c$ is the wave number of mode m and p_r is the momentum of the recirculating beam. R_{ij} is the transfer matrix for the entire recirculation from the cavity exit back to the cavity entrance.

To obtain a value for the current threshold for an entire linac, it is necessary to consider possible interactions of all HOMs acting on a bunch as it exits and returns to a particular cavity, and therefore for a multi-cavity system we use a computer model. The most practical computer code available was found to be the BI code from Cornell [1], as it is convenient to run in batch mode. For all calculations in this paper the HOMs from a 9-cell TESLA cavity [2,3] were used unless otherwise stated.

The BI code is used to search for the current threshold of the instability, the threshold being determined as the minimum value from each HOM from any cavity. It is a tracking code, which calculates the beam position as a function of time and increases the beam current until a threshold is found. The code considers a physical model of the accelerator, in which the bunch train sees a string of cavities, and applies kicks from the HOMs as the bunches pass. The initial HOM characteristics and the lattice of the accelerator are defined by the user.

The HOMs are characterized by their loaded quality factor, which takes into account any HOM damping applied to the cavity. From equation (1) it may be seen that the larger the product $Q_L R/Q$ is, more important the effect on the beam is. Table 1 contains the most important HOM frequencies and their characteristics for the TESLA cavity case.

R/Q (Ω)	Q_L	Freq (GHz)	Polarization (deg)
116.7	3400	1.734	0
116.7	4500	1.734	90
42.2	50600	1.865	0
42.2	26500	1.865	90
58.6	50200	1.874	0
56.7	51100	1.874	90
11.8	95100	1.88	0
11.8	85500	1.88	90
1.2	633000	1.887	0
1.2	251000	1.887	90

Table 1: Characteristic HOMs of a 9-cell TESLA cavity.

To simulate the transverse beam optical transport of the ERL configuration, the Arc-en-Ciel group has developed a code using Matlab [4], whilst the 4GLS group has used ELEGANT [5]. In both cases, the optical functions have been adjusted to optimise the threshold current for a given linac configuration.

The Arc-en-Ciel code is based upon the calculation of the transfer matrix of the beam envelope for each accelerator component: the quadrupoles are approximated by thin lenses surrounded by two straight sections; the straight lengths are half a quadrupole length. The arcs

are considered as a linear transport with imposed conditions at their entrance and exit. The beta functions are the same at the entrance and at the exit of the arcs while the alpha functions are of opposite sign to keep overall lattice symmetry. The Matlab code allows the parameters of the accelerator and the resulting optical functions to be adjusted. Simultaneously the transfer matrix calculated for each element is written into the lattice file which acts as input to BI.

The ELEGANT tracking code was used to calculate the lattice functions for 4GLS. It uses the Rosenweig-Serafini/Chambers definition for the cavities [5], and thick lenses were used for the quadrupoles between the linac modules. To execute BI a script was written to produce the input files required for the cavities, magnets and recirculation and also to run BI.

3 Linac Focusing Scheme

A graded-gradient focusing scheme [6] is chosen by both 4GLS and Arc-en-Ciel. In this scheme the focusing magnets are always matched to the lower-energy beam at any particular location through the ERL modules, and therefore the magnets are matched to the accelerating beam for the first half of the linac and the decelerating beam for the second half. The 4GLS group has studied the behaviour of having either a singlet, doublet or triplet of quadrupoles between each linac module, and the resulting effect upon the BBU instability threshold current. The Arc-en-Ciel team has utilised a triplet (after a brief comparison with the doublet case) and has studied the case of different repetition rate with either one or two recirculations. For the triplet case both Arc-en-Ciel and 4GLS have used an arrangement where the focusing strength of the triplet quadrupoles is $-k/2$, k , $-k/2$ through the triplet.

3.1 4GLS

The number of quadrupoles in the linac focusing scheme has been investigated as part of the 4GLS [7] design. One, two or three quadrupoles have been placed between each module and the focusing setup arranged to give approximately equal Twiss values in each plane. With one quadrupole between each module the polarity of the magnets were reversed from module to module; with two quadrupoles the focusing arrangement was $k/-k$; with three quadrupoles the arrangement was $-k/2$, k , $-k/2$. For the singlet and doublet cases two intermodule spacings were studied - 1.4/2.0 m for the singlet and 1.7/2.0 m for the doublet – to see how much of an effect it had. For each focusing case the variation of threshold current with k , and therefore phase advance between the modules, was determined for k values between 1 and 5 m^{-2} .

These three schemes gave significantly different results: the singlet produced the worst result with a threshold peaking at 16 mA for both the short and long cases. The triplet gave a broader spread (i.e. good threshold region) than the other two options, with a threshold above 30 mA when $2.15 < k < 3.7$, however only giving a maximum threshold current of 56 mA. The doublet had a slightly narrower peak with a threshold above 35 mA over a range of $1.2 < k < 2.9$ and a peak of 98 mA for the short case and remains above 35 mA for a range of $1.2 < k < 2.4$ and a peak of 85 mA for the long case. The singlet, doublet and triplet results can be seen separately in figs. 3, 4 and 5 with figs. 3 and 4 showing both the short and long cases on the same plot.

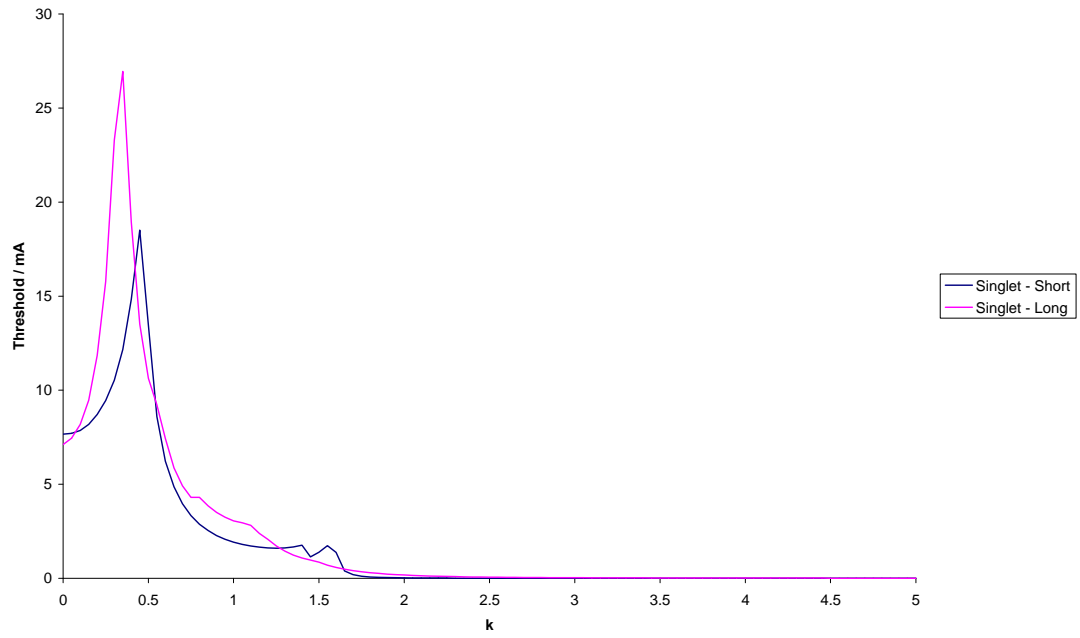


Figure 3: Singlet Case, Current threshold vs. k value.

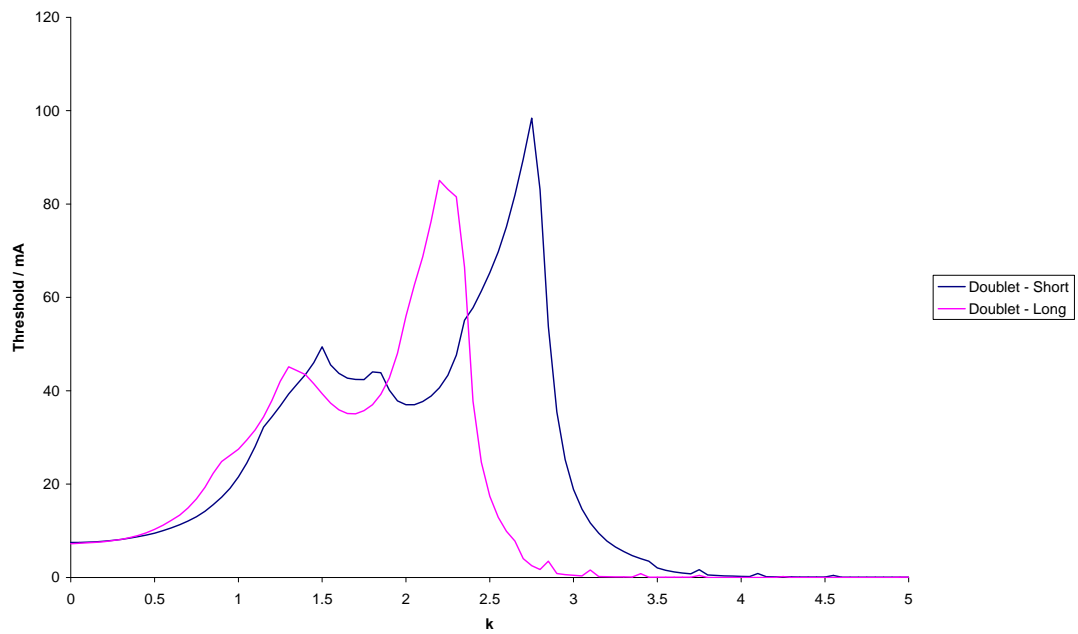


Figure 4: Doublet Case, Current threshold vs. k value.

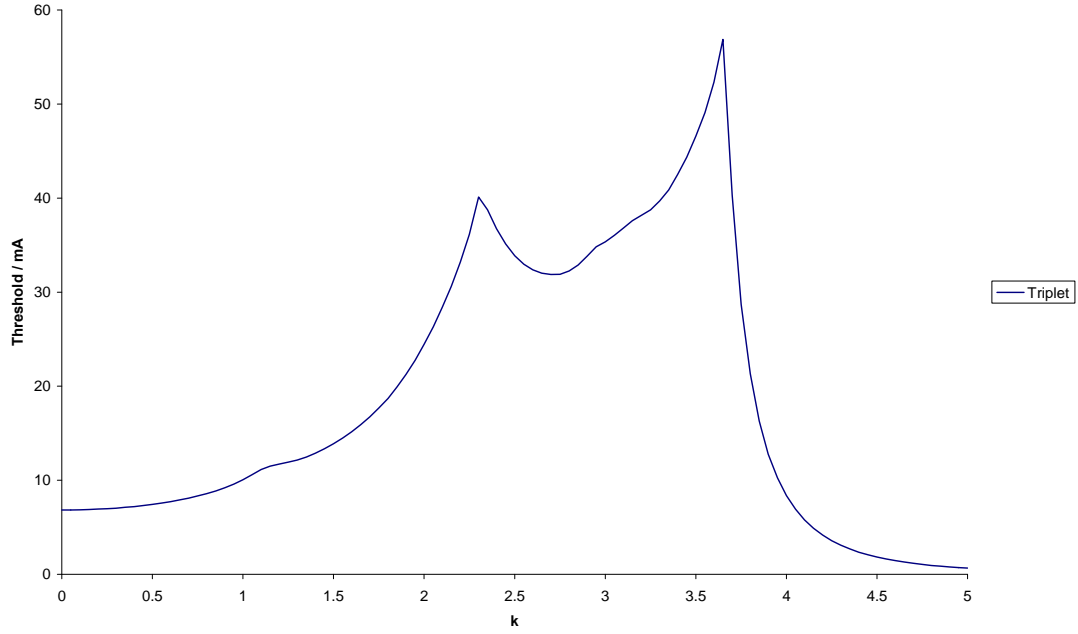


Figure 5: Triplet Case, Current threshold vs. k value.

When the distance between the modules is decreased to accommodate the lesser number of magnets, instead of replacing them with drift tube, the basic shape of the curve stays the same but the threshold increases slightly and shifts along the k axis: this shift is due to the corresponding change in recirculation path length. This effect is best seen in figs. 3 and 4 where the different doublet and singlet models are compared. To compare the focusing schemes the short case is plotted in fig 6 and the long case in fig 7.

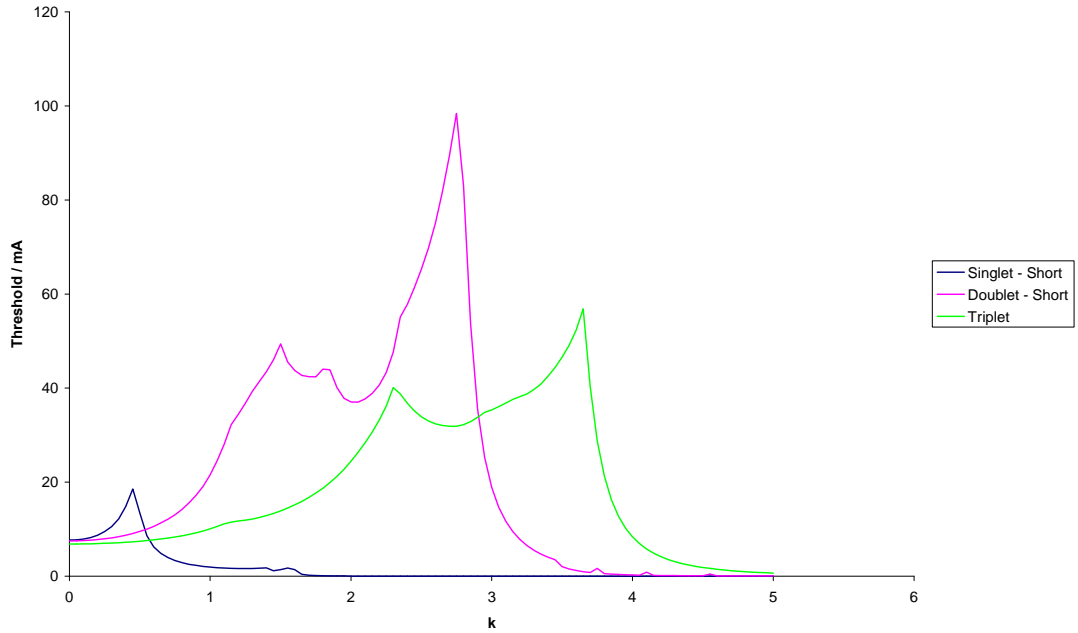


Figure 6: Threshold for changing k value with gap between modules decreasing.

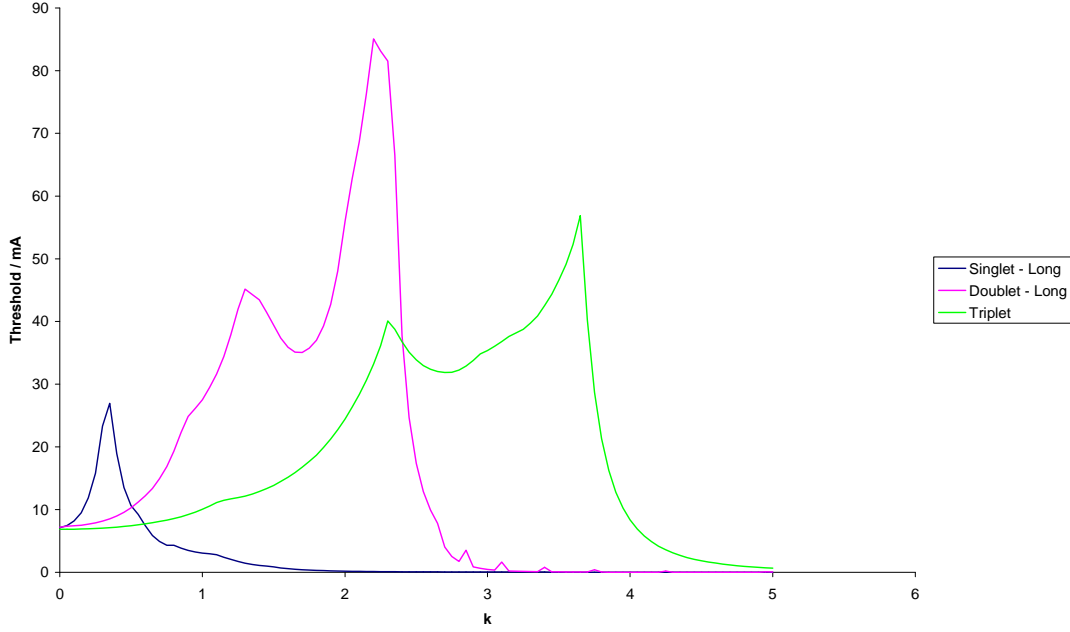


Figure 7: Threshold for changing k value with gap between modules staying the same.

As may be seen from the last two figures, the best option appears to be a short doublet focusing scheme giving a relative broad current threshold which peaks at 98 mA. However, to improve on this threshold we examine addition schemes below, such as improved HOM dampers and couplers, skew quadrupole BBU compensation [8, 9, 10] and 7-cell TESLA cavities.

3.2 Arc-en-Ciel

3.2.1 One-pass recirculation

The Arc-en-Ciel graded-gradient focusing scheme uses a triplet of quadrupoles between each linac module with a focusing arrangement of $-k/2$, k , $-k/2$. Simulations with a simplified design considering a 100 MeV to 1 GeV linear accelerator have been performed with one recirculation pass. These simulations have investigated the evolution of the BBU current threshold as a function of the focusing strength and confirm that the graded-gradient scheme is most appropriate. Figure 8 illustrates the energy variation along the acceleration and the corresponding Beta functions. The functions during acceleration are symmetric compared to the functions during deceleration and vary between 2 and 55 m.

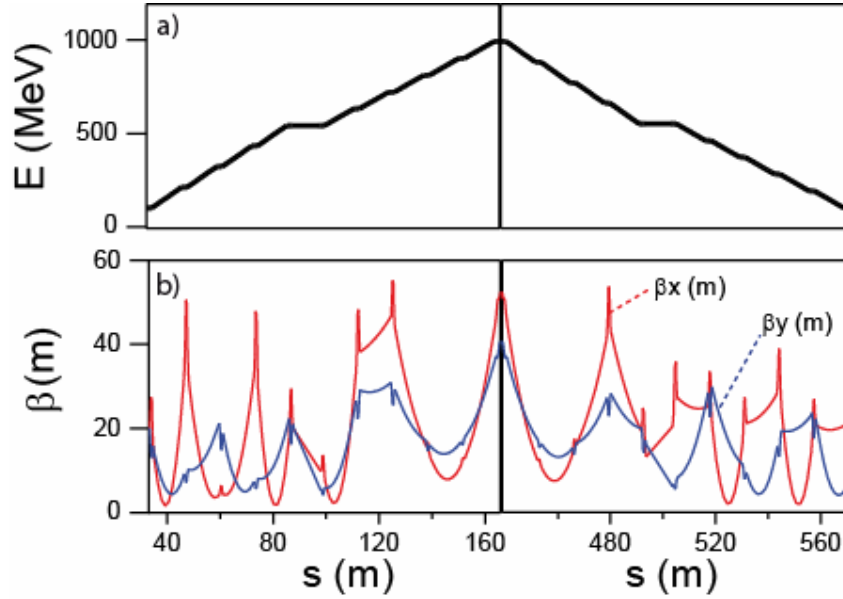


Figure 8: a) Energy, b) Beta function along the accelerator. Triplet parameters: length between quadrupoles is set at 0.3 m, the quadrupole lengths at $L_{qp} = 0.3$ m and the focusing strength at $k=2.5 \text{ m}^{-2}$.

The maximum bunch charge in the ERL configuration of 1 nC giving an average current of 1 mA for a 1 MHz repetition rate and 100 mA for a 100 MHz repetition rate.

Figure 9 shows the threshold as a function of the quadrupole focusing strength. It shows that for the 1 mA scenario the BBU instability will not limit ERL operation. However for the 100 mA case the choice of k will be critical.

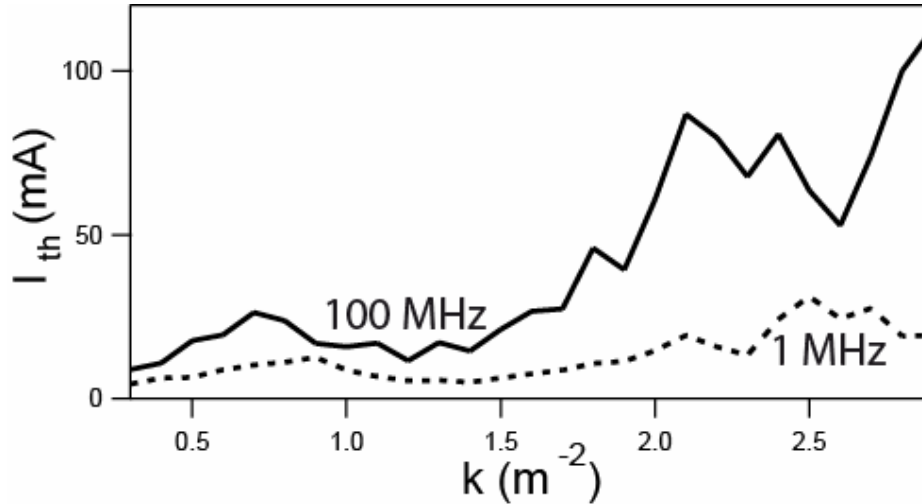


Figure 9: Average threshold current of the instability as a function of the quadrupole strength. Triplet parameters: length between quadrupoles is set at 0.3 m, the quadrupoles length at $L_{qp} = 0.3$ m.

3.2.2 Two-pass recirculation

The main difficulty of a multipass recirculation ERL is to match the focusing for different particle energies. In the case of Arc-en-Ciel, two recirculations are needed to attain

2 GeV beam with approximately a 1 GeV linac acceleration per pass. At the beginning and end of the linear accelerator, the focusing has to be adjusted for a 110 MeV, 1 GeV and 2 GeV electron beam. The quadrupole gradient should be sufficient for a 2 GeV beam (to keep beta functions below 100 m), and not too much for a 110 MeV and a 1 GeV beam.

Some simulations using a Matlab code have been performed to find a graded-gradient focusing solution with beta functions below 100 m. For constant quadrupole strength along the first half of the linear accelerator (first pass for increasing the energy from 110 MeV to 1 GeV), only one value of the quadrupole strength gives the desired beta functions. This configuration is shown in fig 10. As expected, the beta functions are much higher at 2 GeV. The threshold current of BBU instability is 22 mA for 1 MHz repetition rate and 30 mA for 100 MHz repetition rate. With two recirculations ERL at 2 GeV and a constant strength graded gradient focusing scheme, the BBU instability limits the average current to 30 mA instead of the 100 mA desired. Further work on optical and HOM damping schemes will improve this threshold.

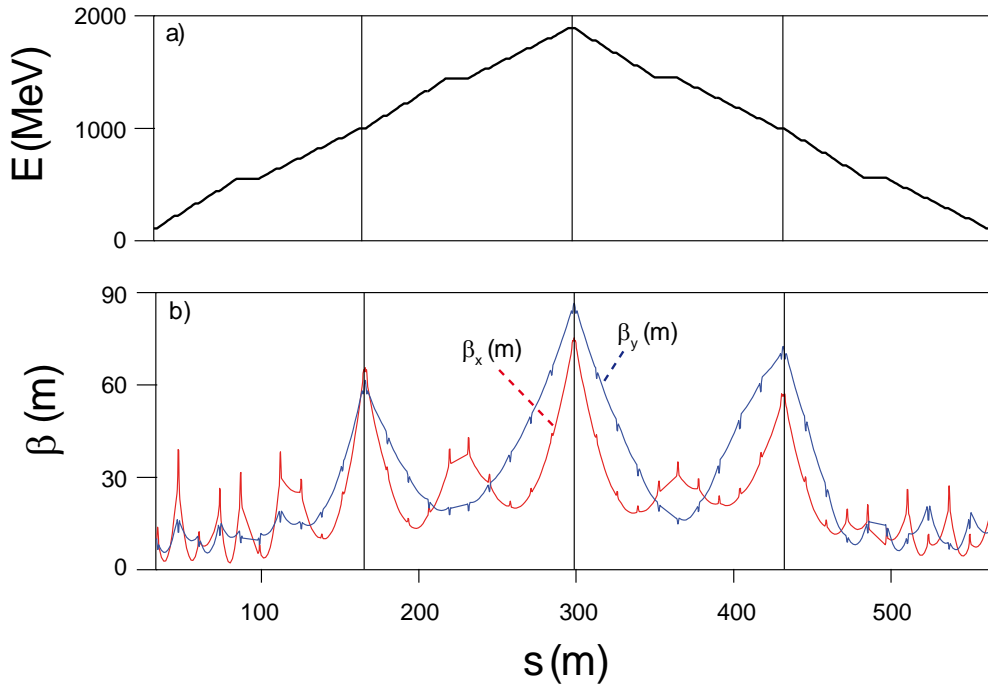


Figure 10: a) Energy, b) Beta function along the accelerator in the second accelerating pass of Arc-en-Ciel. Parameters: Triplet parameters: length between quadrupoles is set at 0.3 m, the quadrupole lengths at $L_{qp} = 0.3$ m, the focusing strength $k=2.5 \text{ m}^{-2}$.

3.3 Comparison

At a first glance the 4GLS and Arc-en-Ciel machines appear to be very similar. However investigation of the BBU instability has highlighted important differences. The setup of the quadrupoles and the higher focusing strength investigated on 4GLS has lead to the choice of two quadrupoles between each module. Arc-en-Ciel uses three due to the multiple passes required to achieve 2 GeV which forces stricter constraints on the parameters influencing the threshold. To first approximation the desired 100 mA average current has been achieved for both machines for a given configuration of each accelerator. However each model contains

simplified optics and this threshold can only be achieved for a small set of parameters; further investigation is required

4 Improving the BBU Threshold

4.1 Further investigation of focusing schemes

4.1.1 4GLS Optics Refinement

The previous results in this report have used a non-optimised lattice for the 4GLS recirculation. As the recirculation optics has developed to match overall compression demands, the resulting threshold current decreased considerably. A variation of threshold against k for a doublet focusing scheme is shown in fig 11 below.

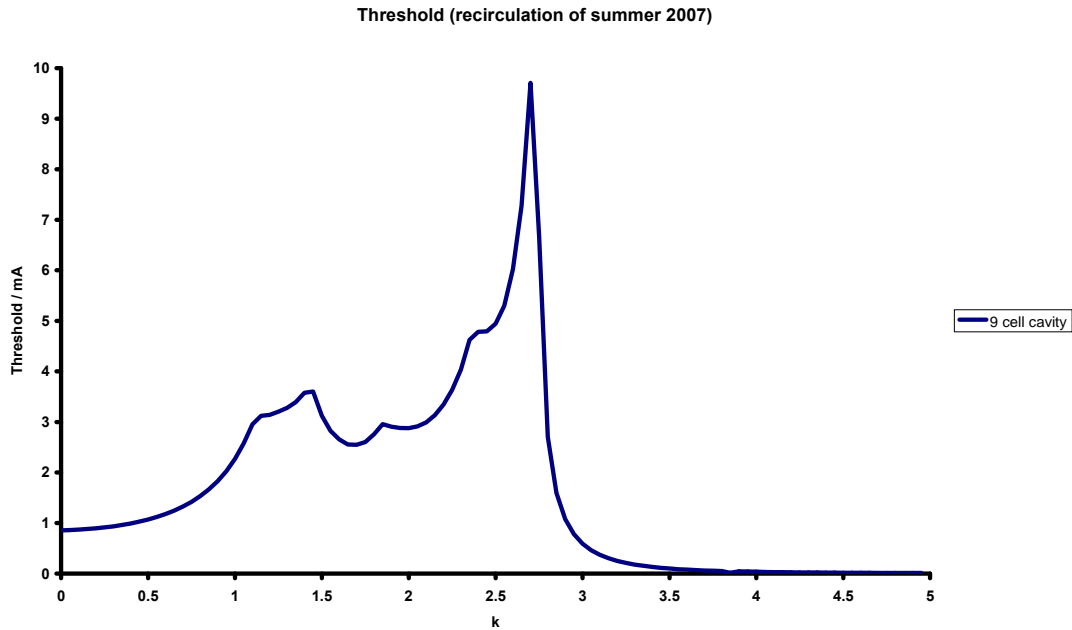


Figure 11: Example 4GLS threshold calculation for modified 4GLS optics.

To improve this threshold, we looked at the effect of a varying recirculation phase advance in each plane, μ_{fx} and μ_{fy} , since

$$R_{12} = \sqrt{\frac{\beta_{ix}}{\beta_{fx}}} \sin(\mu_{fx} - \mu_{ix}) \text{ and } R_{34} = \sqrt{\frac{\beta_{iy}}{\beta_{fy}}} \sin(\mu_{fy} - \mu_{iy}).$$

This produced the curious result (shown in fig 12) where no change was seen in the threshold as μ_{fy} was changed.

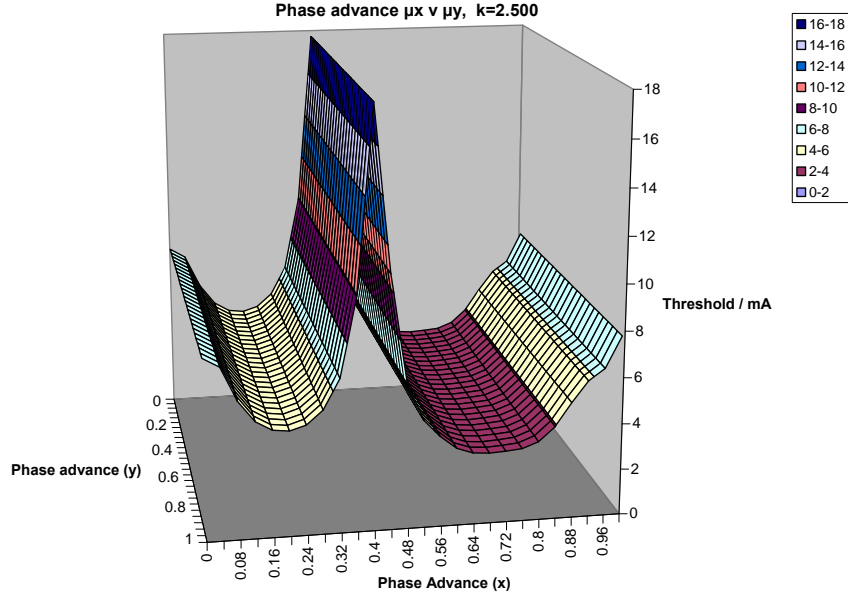


Figure 12: Threshold as a function of phase advance

To study this further, we used the same HOM and Twiss parameters as this lattice, and investigated the effect of a changing R_{12} and R_{34} from each cavity back to itself. For simplicity, we used only one linac module in this model, containing eight cavities as shown in fig 13 below.

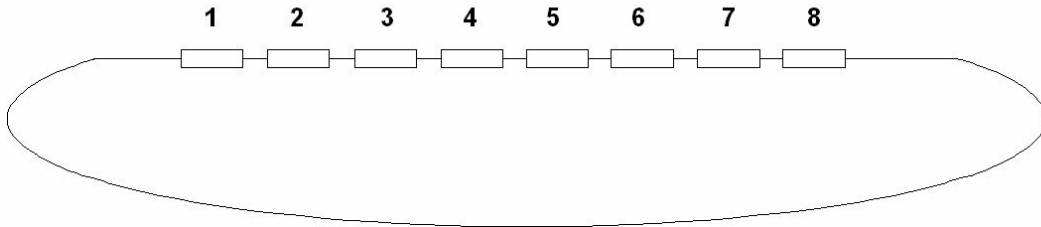


Figure 13: Eight cavity model for phase advance study.

Comparing the values for R_{12} and R_{34} in Table 2 for each cavity, the value of R_{12} can clearly be seen to increase as the Twiss values are propagated.

Table 2: R_{12} and R_{34} for each cavity.

Cavity	R_{12}	R_{34}
1	-17.8284	1.02668
2	-62.2932	4.37928
3	-111.111	8.07217
4	-162.512	11.9709
5	-215.934	16.031
6	-271.17	20.2355
7	-328.154	24.5784
8	-386.885	29.0591

As previously mentioned R_{12} is proportional to μ_{ix} , μ_{fx} , β_{ix} and β_{fx} , and the same is true for R_{34} in the y plane. However, Table 3 contains the Twiss parameters used in this calculation and the values for μ_{ix} , μ_{fx} , β_{ix} , β_{fx} and μ_{iy} , μ_{fy} , β_{iy} and β_{fy} are of similar magnitude but α_{fx} and α_{fy} differ by two orders of magnitude.

Table 3: Recirculation parameters.

R_{12}	R_{34}
$\beta_{ix} = 20.700$	$\beta_{iy} = 50.000$
$\beta_{fx} = 5.930$	$\beta_{fy} = 5.055$
$\alpha_{ix} = 0.530$	$\alpha_{iy} = -2.140$
$\alpha_{fx} = -20.242$	$\alpha_{fy} = -0.314$
$\mu_{ix} = 0.000$	$\mu_{iy} = 0.000$
$\mu_{fx} = 0.720$	$\mu_{fy} = 0.000$

By reducing the value of α_{fx} to 2.242 the value of R_{12} increases at a slower rate which can be seen in table 4.

Table 4: R_{12} and R_{34} for each cavity with new parameters.

Cavity	R_{12}	R_{34}
1	-4.32955	1.02668
2	-8.96736	4.37928
3	-14.7358	8.07217
4	-21.4069	11.9709
5	-28.7874	16.031
6	-36.709	20.2355
7	-45.0223	24.5784
8	-53.5913	29.0591

Equation (1) implies that the BBU threshold current in the transverse instability case is dependant only on R_{12} and R_{34} . This equation is for a single cavity and single HOM and in a multiple cavity system it is clear that the value of $\alpha_{fx}(R_{22})$ and $\alpha_{fy}(R_{44})$ must also be considered; as this effect will be more pronounced as the number of cavity increases.

4.1.2 Arc-en-Ciel

4.1.2.1 One recirculation

As the BBU instability is sensitive to parameters which act on the matrix elements of the recirculation arc, a simulation has been carried out which varies both the phase advance of the optics and the overall length of the arc. As shown in fig 16, the variation of the phase advance reduces the threshold current by a maximum of 17 % in the one recirculation case. This parameter can be used to optimize the threshold current. In this case changing the arc length by seven meters allows 50 mA to be reached instead of 30 mA.

The R_{12} element of the transfer matrix of the arc is changed and it modifies the effect of HOMs on the beam. In addition the total length should be adjusted. This can be crucial if operation at a 2.5 MHz repetition rate is desired, in which case the arc length must be adjusted to give an overall 5 MHz repetition rate in the 1 GeV arc for two recirculations.

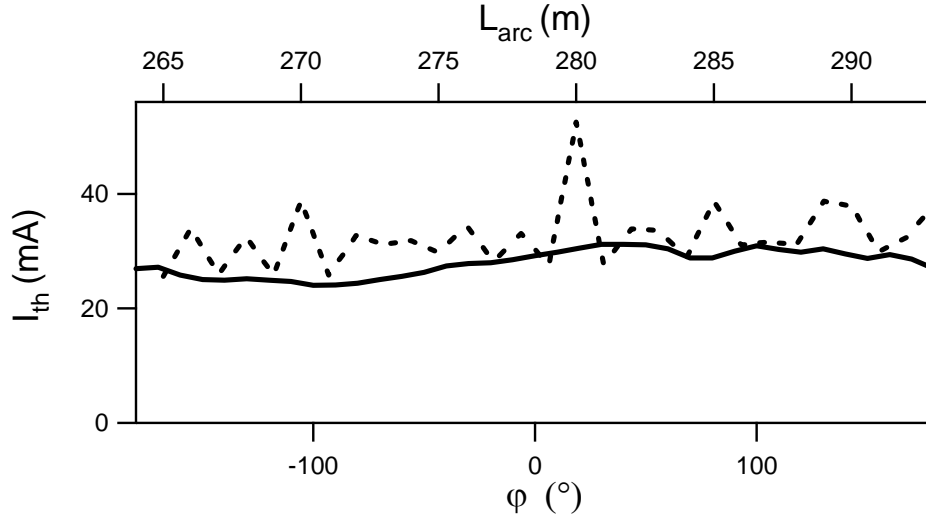


Figure 16: Average threshold current of the instability as a function of the phase advance in the recirculation arc ϕ (plain line) and of the length of the arc L_{arc} (dashed line). Triplet parameters : length between quadrupoles is set at 0.3 m, the quadrupole lengths to $L_{\text{qp}} = 0.3$ m, the focusing strength is $k=2.5 \text{ m}^{-2}$, the repetition rate is 1 MHz, and the arc length is $L_{\text{arc}}=273$ m.

The transfer matrix from element to element also has to be optimized. In the standard case, a graded-gradient scheme has been chosen with a quadrupole strength constant along the first half of the accelerator (see fig. 17a). As a consequence the minimum and maximum gradients are:

$$\begin{aligned} G_1 &= k/cq\sqrt{E_1^2 - E_0^2} \\ G_2 &= \alpha k/cq\sqrt{E_1^2 - E_0^2} \end{aligned} \quad (2)$$

The α coefficient was modified from 0.2 to 1.8 in order to optimize the optics for the BBU. The standard case corresponds to $\alpha = 1$. Figure 17b shows the threshold current versus the quadrupole strength k ; the data take into account a configuration with beta functions less than 80 meters. The maximum threshold is obtained when $\alpha=1.1$ but it is only achievable for a small range of values. Using $\alpha=1.0$ gives a smaller threshold but allows for a greater range of beta functions, and thus more flexible optics.

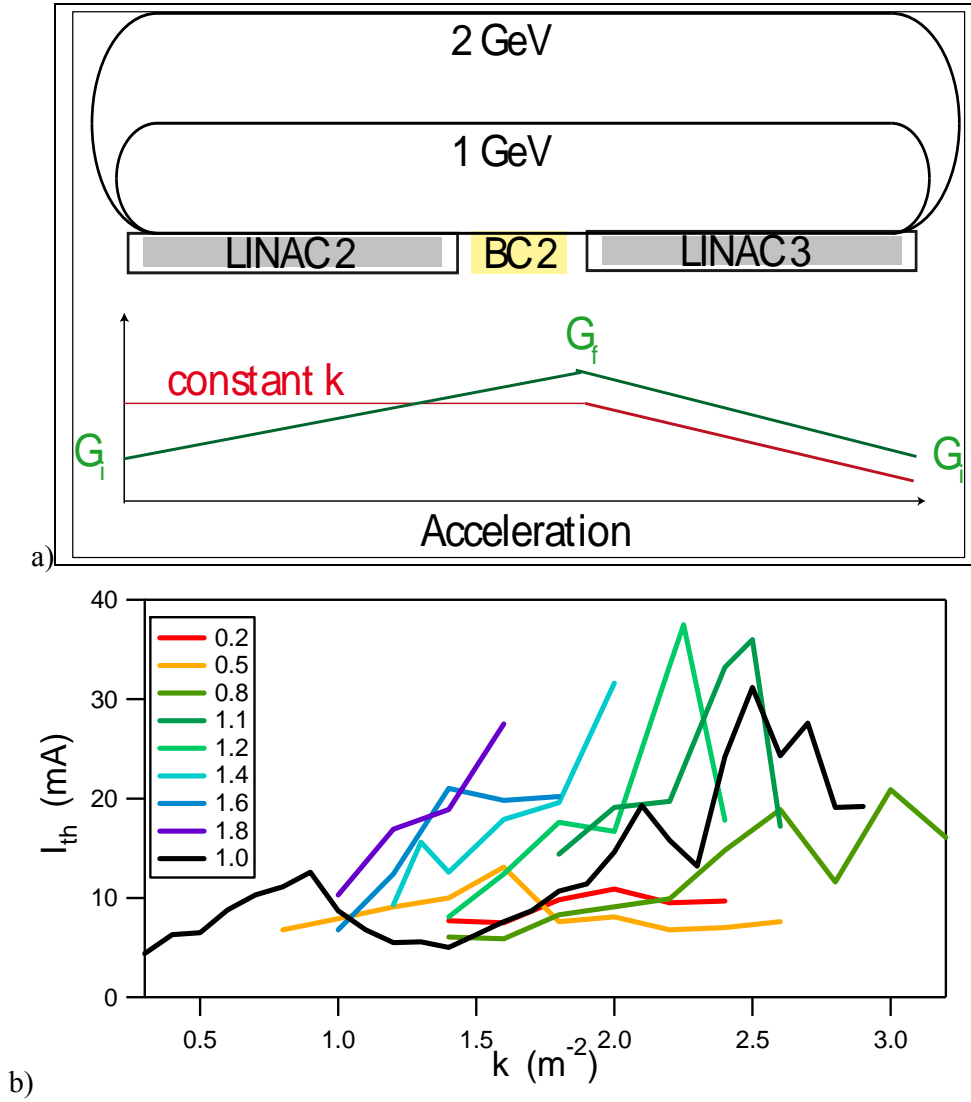


Figure 17: a) Schematic representation of the graded gradient optics. b) Average threshold current of the instability as a function of quadrupole strength for different quadrupole gradient Triplet parameters : length between quadrupoles is set at 0.3 m, the quadrupoles length at $L_{qp} = 0.3$ m, the deflexion parameter is $k=2.5$ m^{-2} , the repetition rate is 1 MHz, and the arc length is $L_{arc}=273$ m.

In summary, to maximise the threshold current for a 1 GeV ERL with one recirculation:

- the phase advance of the electrons in the arc should be optimized
- the arc length should be optimised in the BBU instability and compromise should be made with the desired temporal structure of the synchrotron radiation in the arc.
- The graded gradient scheme should be matched so the quadrupole strength constant along the first part of the accelerator.

4.1.2.2 Two recirculations

In the single recirculation case, the phase advance of the electrons in both arcs has been optimised to maximise the threshold current. First the phase advance in the 1 GeV arc has

been fixed at -150° and the phase advance of the 2 GeV arc has been varied. As illustrated in fig 18, this adjustment is necessary because it allows an increase in threshold current of more than 100 %, from 8 to 20 mA, to be obtained. Then, taking the best phase advance of the 2 GeV arc the 1 GeV arc is then optimised. An improvement from 20 to 22 mA is achieved (see fig 18) for the 1 MHz repetition rate case. Further improvement requires longer arcs.

The optics focusing has been modified by changing the α coefficient as in equation (2). The quadrupole strength was increased from 2.3 to 2.5 m^{-2} for $\alpha=1.1$ but the resulting threshold current was smaller, 18 mA, than in the previous case (22 mA).

Other optics schemes were investigated including a constant gradient design where the quadrupole strength remains constant along the entire linear accelerator for the first pass but no improvement on the BBU threshold was made. The graded-gradient scheme with constant quadrupole strength along the first half of the linear accelerator appears to be the best configuration to minimize the effects of the BBU instability upon average current.

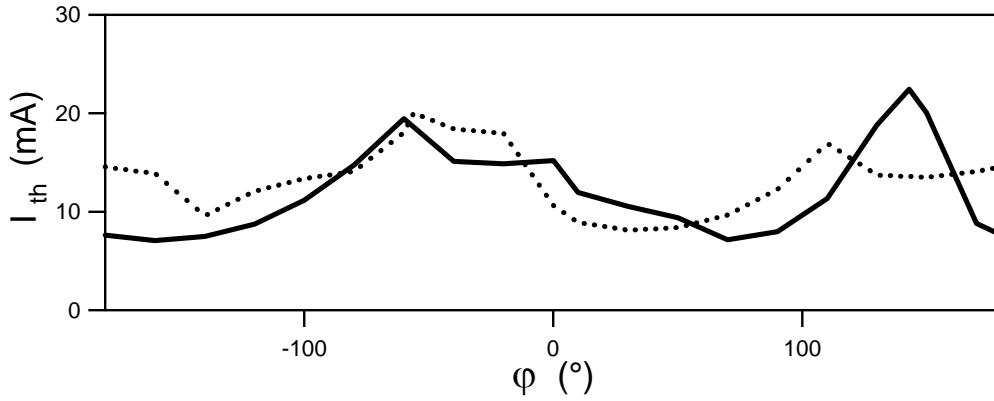


Figure 18: Average threshold current of the instability as a function of the phase advance in the 1 GeV recirculation arc (plain line) and in the 2 GeV recirculation arc (dashed line). Triplets parameters : length between quadrupoles is set at 0.3 m, the quadrupoles length at $L_{qp} = 0.3 \text{ m}$, the deflexion parameter is $k=2.5 \text{ m}^{-2}$, the repetition rate is 1 MHz, and the small arc length is $L_{arc}=273 \text{ m}$, and the longer arc length is $L_{arc2}=373 \text{ m}$.

4.1.3 Injection energy

For most ERL projects the injection energy is 10 MeV. As a consequence, some simulations have been done on the Arc-en-Ciel scheme with an injection energy of 10 MeV instead of 110 MeV. The optics was to be slightly modified with a quadrupole strength set at 2.55 m^{-2} and $\alpha=1$ for the graded-gradient configuration. In this case, for a 1 MHz repetition rate the threshold current of the BBU instability is 3.6 mA, and is 8 mA for 100 MHz repetition rate. For both cases, the threshold current is lower than the case with 110 MeV injection energy. For the 100 MHz case and 110 MeV injection energy, there is a reduction from 30 mA to 8 mA for a 10 MeV injection energy, so further studies will be obliged to master the focusing scheme to control the BBU instability.

4.2 Cavity design

A TESLA nine-cell cavity design was used for the BBU calculations presented above, since the seven-cell cavity design envisaged for use on 4GLS was not available at the time of these simulations. 4GLS will utilise a seven-cell cavity design to allow the inclusion of HOM dampers and therefore to improve the possible circulating current. Each cavity has two HOM dampers - one each side of the cavity - with differing radii to enable broadband HOM suppression. This resulted in the consideration of two different seven cell models; one with an iris before the larger beam pipe, fig 19a, and one without, fig 19b.

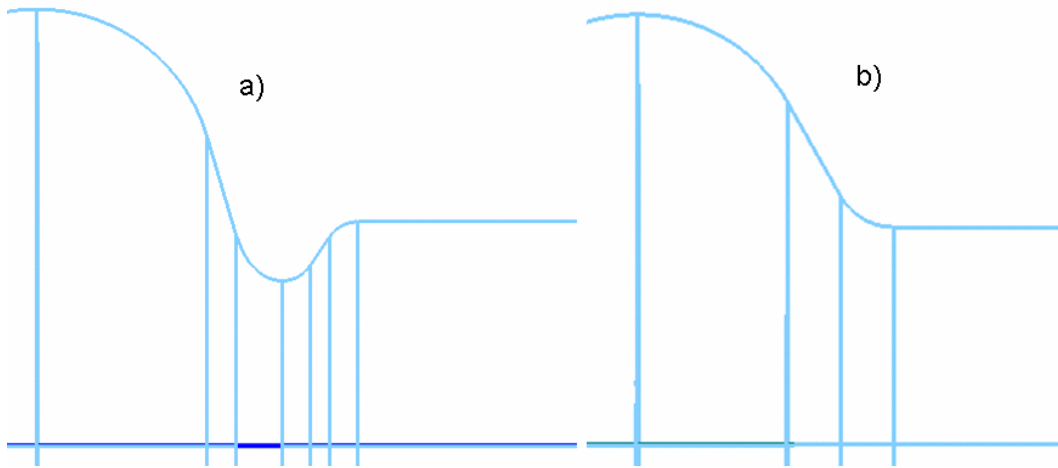


Figure 19: Cavity to beam pipe transitions with a larger beam pipe a) with an iris and b) without an iris

Removing the iris allows more HOMs to propagate to the damper and therefore would reduce the BBU threshold current; this must be balanced against the reduction in the fundamental mode's Q and impedance. The threshold for these two 7-cell cavities has been calculated for a range of quadrupole focusing k values and they are compared to the nine-cell TESLA cavity in Figure 20 below.

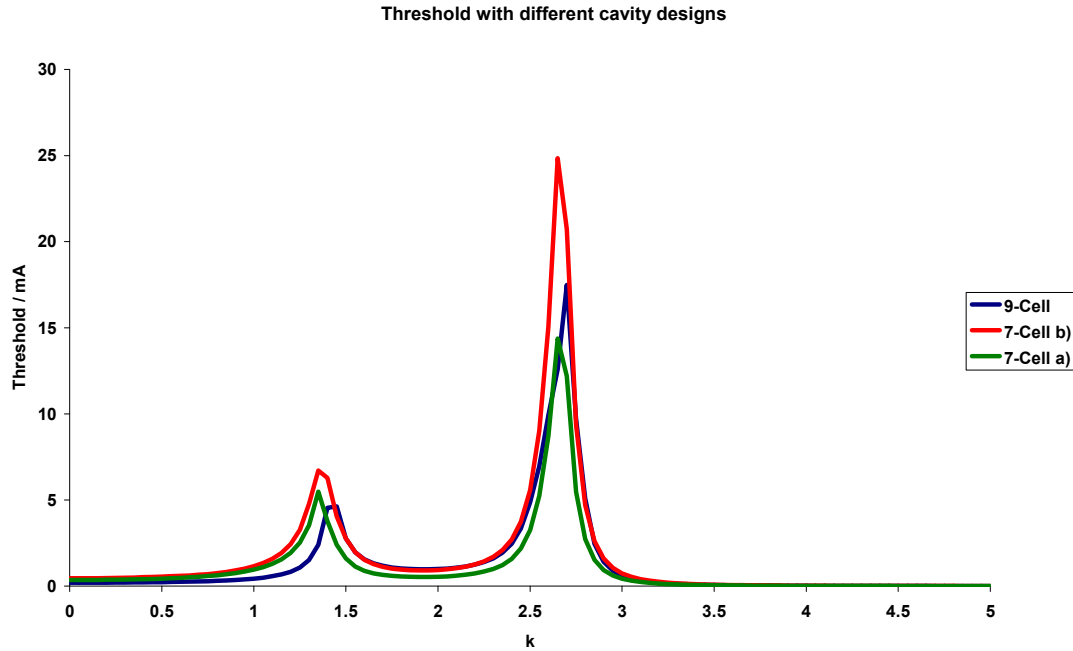


Figure 20: Threshold calculation for a nine-cell cavity and seven-cell cavities, with and without an iris transition.

A paper by G. Hoffstaetter states [11] that considerable improvements in threshold current can be achieved by splitting the degeneracy of the dipole HOMs within a cavity. It is suggested that this can be achieved by making the cavity slightly elliptical, although the degree of ellipticity is not specified in the paper. Instead of making these cavities elliptical, a small dent in the cavity shape could produce the same effect. If such a method proves successful in producing a reasonable increase in BBU threshold, the cavities would be made elliptical rather than deforming them in the way shown below. A model of a seven-cell TESLA cavity was created in CST Microwave Studio [12]. From this model three different options were investigated: these were

- a) Making a dent in the same position in each cell
- b) Alternating the position of the location of the x and y plane
- c) Rotating the dent

A schematic representation of these deformation options is given in Figure 21 below.

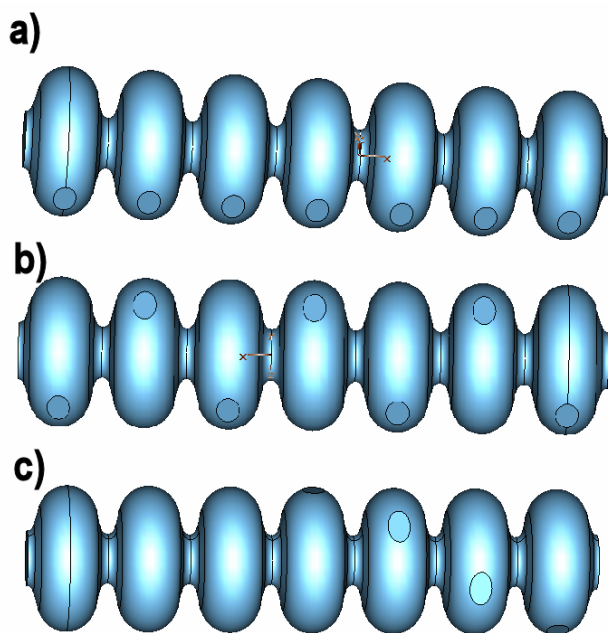


Figure 21: Different cavity designs.

The Q and R/Q of these cavities is shown in figs 22 and 23 below. For comparison the Q and R/Q of the HOMs of a non-optimised seven cell cavity are also plotted.

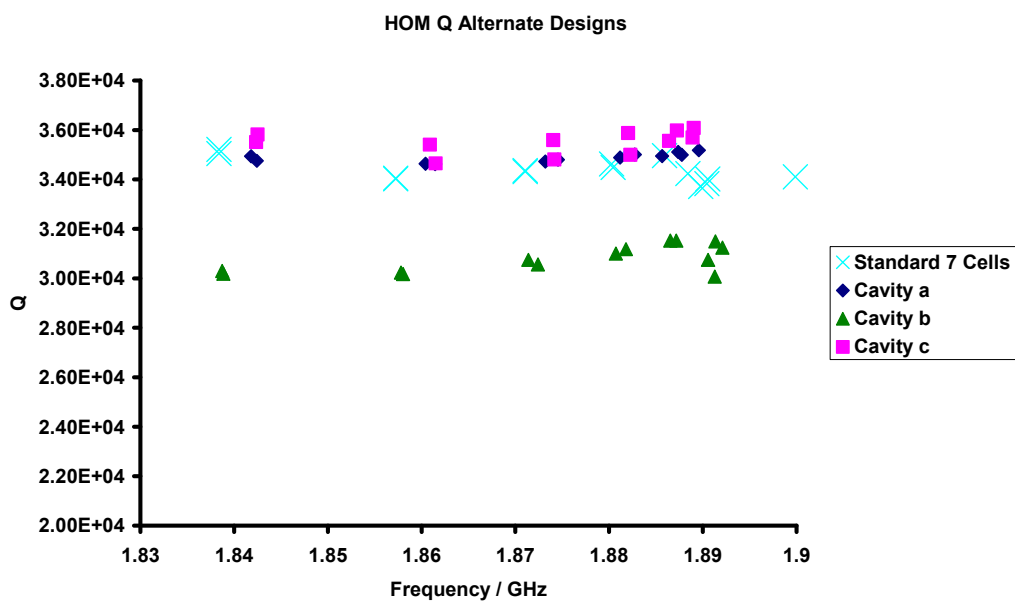


Figure 22: HOM Q for alternate cavity designs.

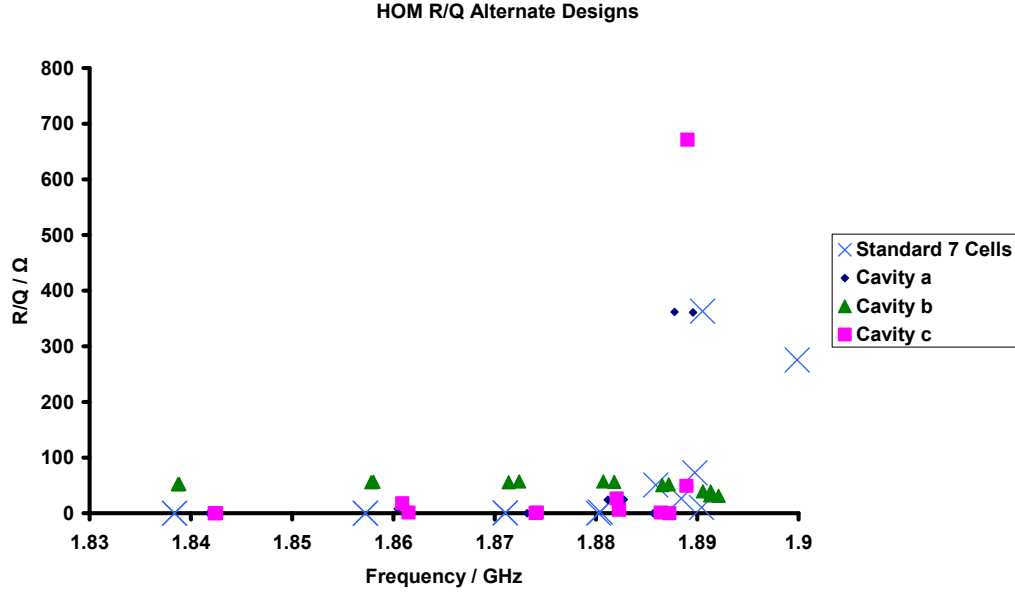


Figure 23: HOM R/Q for alternate cavity designs.

The Q of the HOMs for cavity 'b' is substantially lower than the other cavities, however fig. 23 shows that this cavity's HOMs have slightly larger R/Q values. Using an arbitrary recirculation and the HOMs from each of the cavity models, the BBU current threshold was calculated, and the results are given in table 5. From this table it can be seen that the rotational deformation gives no improvement in comparison to a standard cavity. A deformation only in a single plane (here the x plane) sees the threshold almost double. Alternately deforming the cavity in the x and y planes gives an order of magnitude increase.

Table 5: Threshold of alternate cavity designs.

Type of Cavity	Threshold / mA
7-cell cavity	17.9
7-cells as in Fig. 3a	33.1
7-cells as in Fig. 3b	254.9
7-cells as in Fig. 3c	17.8

The frequency difference of the degenerate modes was not found to increase with the squeezing of the cells. The frequency shift was found to be of the order of a few hundred kHz in the majority of cases; the greatest contribution to the increasing of the threshold for these cavities was found to be lowering the HOM R/Q. It is clear from these plots, and table 5, that the cavity deformed in x and y should be examined in future work to show whether it is not just an effect of this particular cavity model, but whether it is generally true for other cavity designs. This may be achieved by further simulations with CST Microwave Studio, modelling the cavity in other available codes, and by using perturbation theory to examine the problem analytically.

4.3 Review of Other Methods

4.3.1 Rotation & Reflection

Rotation and reflection of the beam phase space within the recirculation optics may increase the BBU threshold current. Optical methods for BBU suppression couple the optics in the x and y planes, and are typically calculated assuming one cavity and one HOM; this may be an acceptable assumption for a small machine with only a handful of powerful HOMs. However, in a large machine this assumption is unlikely to be true, and a setup which may neutralise a destructive HOM, in say the first cavity, could exacerbate a troublesome HOM in a later cavity. With the large number of cavities (> 20) and HOMs (> 10) in a medium-to-large machine, finding a solution that fits all HOMs may be unlikely. This has been discussed in reference [11] and roughly quantified for both coupled and uncoupled optics solutions. A cavity containing two HOMs is used as an example to demonstrate that for uncoupled optics the threshold increase is inversely proportional to the HOM Q, from the threshold equation (1). However, when the optics are coupled the threshold increase is proportional to \sqrt{Q} . Coupling the optics therefore decreases the benefit of lower the cavity HOM Qs using mechanical means such as deformation. Of these two schemes, reflection will be the easiest to implement but will only be effective when the HOMs are oriented in the x or y plane; reflection is when the horizontal and vertical phase spaces are exchanged in a plane at 45 degrees to the horizontal axis. Rotating the phase space by 90° will suppress BBU from those HOMs with arbitrary orientations, but it is then necessary to have $R_{14} = -R_{32} = 0$. This method would create a scenario where the bunch will be unable to recouple with the HOM that initially caused the deflection. Reference [8] states that a pure rotation in the optics will be highly sensitive and require a considerable amount of effort to achieve.

4.3.2 Feedback and Feedforward

Three methods exist to damp the HOMs via feedback. In the first method the HOM power from a cavity is measured through the HOM coupler; the phase of this signal is then shifted by 180° and amplified, then sent through a bandpass filter to ensure only the required HOM frequency is transmitted, before being sent back through the HOM coupler. A factor of 4 to 5 decrease in the Q of the measured HOM, and a corresponding increase in the threshold

current, has been measured in [13, 14]. This solution will only act on one HOM in a cavity but is effective if applied to the worst HOM.

In cases where there are many problem HOMs, or there is little information about those HOMs, another method of suppression is bunch-by-bunch feedback. This system consists of two BPMs (Beam Position Monitors) separated by 90° of betatron phase and a pair of kickers further downstream, again separated by 90° of betatron phase. The information from the BPMs is used to calculate the required kick to sufficiently damp the oscillation in just one turn of the machine. This will require the kickers to be more powerful than they would be in a circular machine - where this type of system is typically found - where the oscillation can be damped over several turns. For this method to be efficient the BPMs and kickers should be placed where the betatron functions are at their largest.

A further option is injector-based feedforward. The signal from a BPM downstream of the linac is shifted 180° in phase, amplified, and then fed into a kicker in the ERL injection line. The feedback is no longer bunch-by-bunch, as it applies the correction before the bunch reaches the linac for the first pass, but it has the advantage that it no longer requires the power needed at higher energy, and therefore allows cheaper components to be used. One or more of these methods could be used to increase the BBU threshold and future work will examine their benefits.

5 Conclusion

For a simplified set of optics and a restricted set of parameters, the required 100 mA threshold has been achieved for both the 4GLS and Arc-en-Ciel proposals. Further investigation of the problem is planned to achieve the desired threshold over a larger parameter space. The graded-gradient scheme has been found to provide optimal focusing through the linac. However, efforts to increase the threshold will affect many other parts of the machine and these will need to be taken into account. They include:

- Local R_{ij} value
 - The focusing optics should better investigated to ensure R_{ij} is which increases the BBU threshold.
- Arc length – altering:
 - The temporal structure of the radiation from the arc
 - The building design and size.
- Cryomodule design - with changes to:
 - HOM extraction
 - Increasing the damping and therefore the heat load.
 - Module length.
 - Placement of focusing quadrupoles.
- Feedback/Feedforward
 - By damping the worst HOM in each cavity or module, by inputting power into the cavity at the same frequency as this HOM but 180° out of phase.
 - Feedback system to kick the beam at the point where the beta functions are highest.
 - Feedforward to kick the low energy beam before the problem occurs.
- Rotation or reflection of the beam
 - Will require effort to produce a set of skew optics that will only increase this threshold, whilst not affecting other aspects of the recirculation optics.

This report shows that control of the BBU instability can be achieved to the desired level, but further work is desired to achieve a greater range over which this threshold is achievable; future options for the ERLs could envisage higher operating currents.

6 References

- [1] I. Bazarov, "BI - Beam Instability Code" <http://www.lns.cornell.edu/ib38/bbu>
- [2] S.M. Gruner et al. (2001), 'Study for a proposed Phase I Energy Recovery Linac (ERL) Synchrotron Light Source at Cornell University', CHESS Technical Memo 01-003 and JLAB-ACT-01-04.
- [3] J. Sekutowicz (1994), 'Higher order mode coupler for TESLA', TESLA94-07, DESY, Hamburg, Germany.
- [4] matlab more information available at <http://www.mathworks.com/>
- [5] elegant tracking code, more information available at http://www.aps.anl.gov/Accelerator_Systems_Division/Operations_Analysis/software.shtml
- [6] G. Hoffstaetter, I. Bazarov, "Beam Break Up Instability Theory for Energy Recover Linacs", Phys. Rev. ST Accel. Beams, **6**, 054401 (2004)
- [7] "4GLS Conceptual Design Report", CCLRC Daresbury Laboratory. (2006), available at www.4gls.ac.uk.
- [8] D. Douglas, "Reflections on Rotators, Or, How to Turn the FEL Upgrade 3F Skew Quad "Rotator" Into a Skew Quad Rotator" Jlab technical note, JLAB-TN-04-023.
- [9] D. Douglas, "Operation of the FEL Upgrade with Skew Quad Reflection and Rotation" Jlab technical note, JLAB-TN-04-025.
- [10] D. Douglas, "A Skew-Quad Eigenmode Exchange Module (SQEEM) for the FEL Upgrade Driver Backleg Transport" Jlab technical note, JLAB-TN-04-016.
- [11] G. Hoffstaetter, I. Bazarov, C. Song, Phys. Rev. ST Accel. Beams **10**, 044401, (2007).
- [12] CST Microwave studio. More information available at www.cst.de
- [13] C. Tennant et al, "Experimental Investigation of Beam Breakup in the Jefferson Laboratory 10 kW FEL Upgrade Driver", Proceedings of PAC'05, Knoxville, Tennessee, USA (2005)
- [14] C. Tennant et al, "Methods for Measuring and Controlling Beam Breakup in High Current ERLS" Proceedings of Linac'04, Lübeck, Germany (2004)